DOI: 10.6060/mhc235118s

N-Oxyethylimidazolium Calix[4]arenes and Thiacalix[4]arenes: Difference in Solubilization Property and Detection of Adenine-Containing Nucleotides

Elza D. Sultanova,[a@] Bulat Kh. Gafiatullin,[a] Evgeny A. Ocherednyuk,[a] Ramilya I. Garipova,[a] Anastasia A. Volodina,[a] Amina G. Daminova,[a] Vladimir G. Evtugyn,[a] Vladimir A. Burilov,[a] Svetlana E. Solovieva,[b] and Igor S. Antipin[a]

[a]*Kazan Federal University, 420008 Kazan, Russian Federation*
[b]*Arbuzov Institute of Organic and Physical Chemistry, FRC Kazan Scientific Center, Russian Academy of Sciences, 420088 Kazan, Russian Federation*
[@]*E-mail: elsultanova123@gmail.com*

Dedicated to Academician of the Russian Academy of Sciences Irina P. Beletskaya on the occasion of her Anniversary

The properties of amphiphilic calix[4]arenes and thiacalix[4]arenes containing the same polar N-tetrahydroxyethylimidazolium groups on one side and alkyl fragments on the other side of the macrocyclic platform are shown. Critical aggregation concentration (CAC) values were studied with three methods: solubilization of Orange OT (a); binding of pyrene (b); interaction with eosin Y (c). Absorbance and emission plots of interaction with eosin Y were effectively calculated by a sigmoidal Boltzmann type function. Different solubilizing ability, interaction with a dianion dye, and selectivity of the of binary system macrocycle–eosin Y respectively to adenosine phosphates (mono-, di- or triphosphate) are shown.

Keywords: Calix[4]arene, thiacalix[4]arene, surfactants, solubilization, sensors for adenosine phosphates.

N-Олигоэтиленгликоль-имидазолиевые производные тиакаликс[4]арена и каликс[4]арена: различие в солюбилизирующих свойствах и обнаружение аденозинфосфатов

Э. Д. Султанова,[a@] Б. Х. Гафиатуллин,[a] Е. А. Очереднюк,[a] Р. И. Гарипова,[a] А. А. Володина,[a] А. Г. Даминова,[a] В. Г. Евтюгин,[a] В. А. Бурилов,[a] С. Е. Соловьева,[b] И. С. Антипин[a]

[a]*Казанский (Приволжский) федеральный университет, 420008 Казань, Республика Татарстан, Россия*
[b]*Институт органической и физической химии им. А.Е. Арбузова, ФИЦ Казанский научный центр РАН, 420088 Казань, Республика Татарстан, Россия*
[@]*E-mail: elsultanova123@gmail.com*

Посвящается Академику РАН Ирине Петровне Белецкой по случаю ее юбилея

Изучена агрегация амфифильных макроциклов на основе каликс[4]аренов в конфигурации конус и тиа[4]каликсаренов в конфигурации 1,3-альтернат с N-олигоэтиленгликоль-имидазолиевыми фрагментами в водной среде. Продемонстрировано, что как образующиеся агрегаты, так и индивидуальные макроциклы обладают способностью солюбилизировать гидрофобный краситель Оранж ОТ. Солюбилизирующая ёмкость существенно возрастает при переходе от каликс[4]ареновой к тиакаликс[4]ареновой платформе. Исследовано взаимодействие каликс[4]аренов и тиакаликс[4]аренов с дианионным красителем Эозином Н методами УФ-видимой и флуоресцентной спектрофотомерии. Методом конфокальной микроскопии изучены размеры образующихся комплексов макроцикл–Эозин Н. Установлено, что размеры агрегатов варьируются от 350 до

750 нм. Показано, что комплексы макроцикл–Эозин Н могут использоваться в роли сенсоров на аденозинфосфаты, причем система тиакаликс[4]арен–Эозин Н проявляет селективность к аденозинтрифосфату.

Ключевые слова: Каликс[4]арены, тиа[4]каликсарены, амфифильные соединения, солюбилизация, сенсоры на аденозинфосфаты.

Introduction

Supramolecular self-assembly systems do not lose their popularity in development and design of versatile materials with wide range of applications.[1,2] Supramolecular chemistry is the area of science that is based on using chemical systems with the spatial organization of molecules via noncovalent interactions and molecular recognition.[3,4] A wide variety of synthetic organic receptors that includes crown ethers, porphyrins, calixarenes, thiacalixarenes and cyclodextrins is permanently in use as molecular receptors since the beginning of molecular recognition chemistry (host–guest chemistry).[5] The mixing structures of macrocycles as building blocks for organized assemblies give new life for supramolecular chemistry.

Calix[n]arene chemistry had been causing an unquenchable interest of researchers from late 1980s to early 2000s, but even now calix[n]arene backbones are still demanded as building blocks of for creation of various functional materials.[6-8] Calix[4]arenes, thiacalix[4]arenes and calix[4]resorcinarenes are the most commonly used platforms among other calix[n]arenes for embedding the variety of guests.[9-11] Consequently, calixarenes represent extremely popular and important bricks for building such diverse areas as molecular and supramolecular systems (rotaxanes, inclusion complexes, solid-state architectures, ionic recognition, catalysis, synthesis of architectures based on nanoparticles, different biological applications, and so on[12-15]). Structure of calixarene derivatives can be modified and changed of its nature by modulating their conformation or by introduction of different amounts and various functional groups.[16,17] The conformation of calixarene and thiacalixarene plays a major role in their properties. The calix[4]arene derivatives in conformation of *cone* accept a more classical amphiphilic structure as micelles with the polar groups at one side of the platform. In contrast, the *1,3-alternate* calix[4]arenes form the shape close to cylindrical structure: their hydrophobic parts are enclosed between polar substituents, and they usually self-assemble to vesicles.[18-20] Amphiphiles based on thiacalixarene show lower aggregation ability and higher solubilization capacity compared to their *cone* classic calixarene. An important role in increasing the solubilization capacity is also played by the size of the macrocycle – the volume of the thiacalixarene platform is 15% greater.[21]

In previous works the solubilizing ability of thiacalixarenes[22] and the usage of classical calixarenes in the recognition of adenosine phosphates by the displacement method (fluorescein as indicator) have been shown.[23] These macrocycles have the same functional groups and length of alkyl groups, namely, N-tetraoxyethylimidazolium thiacalixarene and calixarene bearing butyl/octyl fragments on the lower rim of the macrocyclic platform in *1,3-alternate* and *cone*, respectively. This article discusses and compares the influence of the structure of calixarene platforms on the solubilizing ability in relation to the hydrophobic dye, as well as on the selective recognition of adenosine phosphates. It is shown that the complex based on eosin Y and thiacalixarene is sensitive only to adenosine triphosphate, while the calyxarene–eosin Y complex is sensitive to diphosphate and triphosphate.

Experimental

Orange OT (75%), pyrene (≥98%), eosin Y (≥98%) were ordered from the Sigma-Aldrich. N-Oxyethylimidazolium calix[4]arene[22] and thiacalix[4]arene[21] were prepared following literature procedures. The solutions were prepared using water purified by the Millipore system. The 5,7,11,17-tetra-*p-tert*-butyl-25,27-dioctyl-26,28-dihydroxy-2,8,14,20-tetrathiacalix[4]arene[24] and 1-N-(2-(2-(2-methylethoxy)ethoxy)ethoxy)ethyl)-3-H-imidazolium[25] were synthesized according to the literary method.

The NMR spectra were recorded on Bruker Avance 400 Nanobay (Bruker Corporation, Billerica, MA, USA) with signals from residual protons of $CDCl_3$ solvent as the internal standard. IR spectra in KBr pellets were recorded on a Bruker Vector-22 spectrometer (Bruker Corporation, Billerica, MA, USA). High-resolution mass spectra with electrospray ionization (HRESI MS) were obtained on an Agilent iFunnel 6550 Q-TOF LC/MS (Agilent Technologies, Santa Clara, CA, USA) device in the positive mode. The following parameters were used: nitrogen carrier gas, temperature 300 °C, carrier flow rate 12 $L \cdot min^{-1}$, nebulizer pressure 275 kPa, funnel voltage 3500 V, capillary voltage 5. The UV-vis spectra were recorded on a Shimadzu UV-2600 spectrophotometer (Shimadzu Corporation, Kyoto, Japan) in an optical cell with 10 mm light pass at 298 K. Fluorescence experiments were performed in 10 mm quartz cuvettes and recorded on a Fluorolog FL-221 spectrofluorimeter (HORIBA Jobin Yvon) in the range of 350–430 nm and excitation wavelength 335 nm with 2.5 nm slit for pyrene and at the range of 480–650 nm and excitation wavelength 461 nm with 2 nm slit for fluorescein. The aggregates were visualized by CLMS on an inverted Carl Zeiss LSM 780 confocal laser-scanning microscope (CarlZeiss, Jena, Germany). DLS experiments were performed on a Zetasizer Nano instrument (Malvern Instruments, USA) using a 10 mW 633 nm He–Ne laser; the data obtained were processed with the DTS program (Dispersion Technology Software 5.00). Experiments were performed in DTS 0012 plastic cuvettes (Sigma-Aldrich, USA) at 25 °C.

The electronic absorption spectra of Orange OT were recorded in 10 mm quartz cuvettes on a Shimadzu UV-2700 spectrophotometer in the range of 350-700 nm. For this, solutions of thiacalixarenes of a certain concentration (0–2.25 mM) were added to the crystal dye Orange OT (3 mM), and the system was thermostated for 48 hours at room temperature.

Synthesis of 5,7,11,17-tetra-p-tert-butyl-25,27-dioctyl-26,28-di-4'-brombutyloxy-2,8,14,20-tetrathiacalix[4]arene (4EG-CA-C8). The preparation scheme is presented in Figure S1. A mixture of 1.2 g (1.3 mmol) of 5,7,11,17-tetra-*p-tert*-butyl-25,27-dioctyl-26,28-dihydroxy-2,8,14,20-tetrathiacalix[4]arene, 1.37 mL (12 mmol) of 1,4-dibrombutane, 4.1 g (12 mmol) Cs_2CO_3, and catalytic amount of KI were stirred by refluxed in 50 mL of dry acetone for 30 hours. After it, the reaction mixture was cooled and filtered. The precipitate was dissolved in chloroform (20 mL) and extracted with water (2 × 15 mL). The organic layer was drained by $MgSO_4$, solvent was evaporated under vacuum, the precipitate was washed with ethanol to give a white powder product. Yield: 1.2 g (75 %).

TLC R_f = 0.4 (hexane:ethyl acetate, 4:1). ^{1}H NMR (400 MHz, $CDCl_3$, 25 °C) δ_H ppm: 0.88 (t, *J* = 6.9 Hz, 6H, CH_3), 0.93-1.03 (m, 12H, CH_2), 1.05-1.18 (m, 12H, CH_2), 1.27 (s, 18H, $C(CH_3)_3$), 1.28 (s, 18H, $C(CH_3)_3$), 1.59-1.71 (m, 4H, CH_2), 3.24 (t, *J* = 6.8 Hz, 4H, CH_2Br), 3.79 (t, *J* = 7.9 Hz, 4H, OCH_2), 3.87 (t, *J* = 7.5 Hz, 4H, OCH_2), 7.29 (s, 4H, ArH), 7.33 (s, 4H, ArH). ^{13}C NMR (101 MHz, $CDCl_3$, 25 °C) δ_C ppm: 157.33, 156.96, 145.72, 145.67, 128.52, 128.30, 127.97, 127.46, 127.19, 68.82, 68.15, 34.44, 34.34, 33.51, 32.02, 31.59, 31.53, 31.45, 29.35, 29.82, 28.06, 28.86, 25.96, 22.75, 14.25. IR (KBr) ν_{max} cm^{-1}: 3474 (C-H), 1253 (=C-O), 734 (C-Br). HRMS (ESI) *m/z*: $[M+NH_4]^+$ calculated for $[C_{64}H_{98}NO_4S_4]^+$ 1232.4720, found: 1232.4727.

Synthesis of 5,7,11,17-tetra-p-tert-butyl-25,27-dioctyl-26,28-bis[4-(3-N-2-(2-(2-(2-methylethoxy)ethoxy)ethoxy)ethyl)imidazolium)butyloxy]-2,8,14,20-tetrathiacalix[4]arene (4EG-TCA-C8). The preparation scheme is presented in Figure S2. A mixture of 0.2 g (0.16 mmol) of 5,7,11,17-tetra-*p-tert*-butyl-25,27-dioctyl-26,28-di-4'-brombutyloxy-2,8,14,20-tetrathiacalix[4]arene, 0.48 mL (2.4 mmol) of 1-N-(2-(2-(2-methylethoxy)ethoxy)ethoxy)-ethyl)imidazolium were placed into the glass autoclave 'GlassChem' (CEM ® corporation) and dissolved in 3 mL of dry acetonitrile. An inert nitrogen atmosphere was used for the reactions' implementation. The reaction mixture was heated to 130 °C for 30 h. The progress of the reaction was monitored by TLC (petroleum ether:ethyl acetate 1:4, the resulting salts have R_f = 0). To isolate the target products, the solvent was evaporated and the cake was washed with diethyl ether (2×20mL) and dried in *vacuo* for 8 h. Yield: 0.2 g (74 %). TLC R_f = 0 (MeOH). ^{1}H NMR (400 MHz, $CDCl_3$, 25 °C) δ_H ppm: 0.88 (br.t, 6H, CH_3), 1.03-1.37 (m, 60H, CH_2, $C(CH_3)_3$, $C(CH_3)_3$), 1.59-1.75 (m, 4H, CH_2), 1.78-1.91 (m, 4H, CH_2), 3.36 (s, 6H, OCH_3), 3.48-3.71 (m, 24H, OCH_2), 3.76 (br.t, 4H, OCH_2), 3.84 (br.t, 4H, OCH_2), 3.88 (br.t, 4H, OCH_2), 4.17 (br.t, 4H, NCH_2), 4.59 (br.t, 4H, NCH_2), 7.25 (s, 4H, Ar-H). 7.34 (s, 4H, Ar-H), 7.56 (br.d, 2H, NCH), 7.63 (br.d, 2H, NCH), 10.52 (s, 2H, Imd CH). ^{13}C NMR (101 MHz, $CDCl_3$, 25 °C) δ_C ppm: 156.79, 146.09, 145.86, 137.46, 128.72, 128.25, 127.76, 126.62, 125.09, 123.55, 121.85, 72.02, 70.69, 70.54, 70.45, 70.39, 69.28, 68.90, 67.53, 59.13, 49.75, 49.57, 34.49, 34.36, 31.98, 31.84, 31.53, 31.41, 29.79, 29.09, 28.78, 26.50, 25.90, 22.72, 14.22. IR (KBr) ν_{max} cm^{-1}: 2922 (-C-H), 1751 (-C=N-), 1268 (=C-O-). HRMS (ESI) *m/z*: $[M-2Br]^{2+}$ calculated for $[C_{88}H_{138}N_4O_{12}S_4]^{2+}$ 785.4592, found: 785.4583.

Results and Discussion

Solubility behavior of 4EG-CA-Cn and 4EG-TCA-Cn (n = 4, 8)

Calixarenes / thiacalixarenes with positively charged groups on the upper rim and hydrophobic ones on the lower rim typically form aggregates in aqueous solutions (Scheme 1).[26] Using pyrene as a probe is commonly applied for identification of micellar solutions and is quite effective in studies of the influence of additive ingredients on the micellar properties of nonionic and ionic surface-active agents.[27,28] We observe an increase of intensity of the first peak from 372 nm to 374 nm and the third one from 382 nm to 384 nm that leads to changes in the ratio of pyrene peaks (which is also known as the polarity index[29]). This is obviously caused by the decrease of polarity of the pyrene environment that follows from its solubilization in the hydrophobic calixarene aggregates core. (CAC_{pyr})[30] (Figure S3, Table 1). 4EG-CA-C*n* in a *cone* conformation formed aggregates at lower concentration when compared with thiacalixarenes, which coincides with literature data.[17-19]

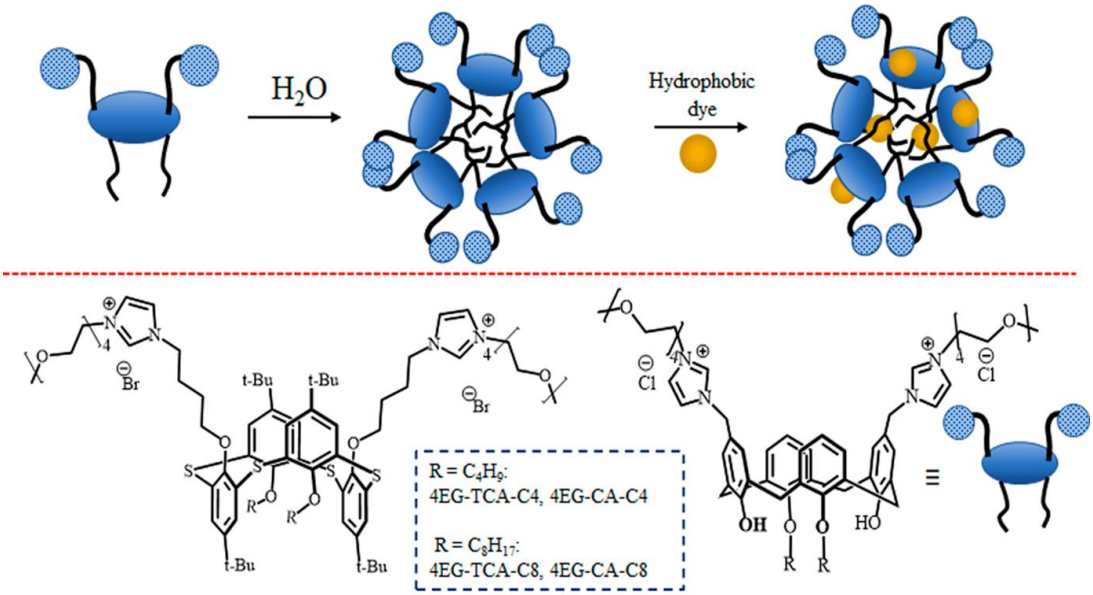

Scheme 1. Structures of the studied macrocycles and schematic representation of its aggregation and solubilization process.

Table 1. CACs and solubilization capacity of 4EG-CA-C*n* and 4EG-CA-C*n* (*n* = 4, 8) identified by dye (Pyrene, Orange OT) micellization method.

System	CAC_{pyr}, mM	CAC_{OT}, mM	S, $mol_{OrangeOT}$/ $mol_{surfactant}$, mM	S_{ind}, mM
4EG-CA-C4	0.031[22]	0.049	14.6	4.4
4EG-CA-C8	0.017[22]	0.028	22.2	31
4EG-TCA-C4	1.650[21]	1.341[21]	8.8[2]	19.2[21]
4EG-TCA-C8	0.146	0.052	33.5	52.5

Solubilization is considered to be a crucial phenomenon of colloidal aggregation that was explored more than fifty years ago (Scheme 1).[31] The dye solubility method is the most suitable for the measurement of solubilization. The ability of macrocycle aggregates to solubilize hydrophobic substrates was tested using the orange OT dye (absorption maximum at 500 nm) (Figure 1). The received data prove the dissolution of orange OT in water but exclusively in the macrocycles presence (CAC_{OT}).[32] As can be seen from Table 1, the CAC_{OT} are close to CAC_{pyr} data obtained by the fluorometric method. The absorption intensity slightly increases at 500 nm in the presence of more lipophilic macrocycles 4EG-CA-C8 and 4EG-TCA-C8 before CAC_{OT}, which indicates the binding of the dye by individual macrocycles. The solubilization capacity of aggregates (S) depends on the number of moles of dye solubilized by one mole of surfactant, is explored by using the equation:[33] $S = B/(\varepsilon_{ext} \cdot l)$, where B is the slope parameter (tangential angle of dependence of the optical density of the dye on the content of surfactant at a concentration above CAC), and ε_{ext} – the extinction coefficient of the dye (ε_{ext} = 17400 $M^{-1} \cdot cm^{-1}$). High solubilization capacity opens the way for the usage of macrocycles as non-viral carriers or drug delivery systems.[34]

However, the formula for calculation of the solubilization capacity does not consider the amounts of the dye absorbed by the separate macrocycle. Although the 4EG3-TCA-C4 macrocycle solubilizes 0.0014 mM of the dye, while the 4EG3-CA-C4 0.0004 mM (from The Beer-Lambert Law). This difference is due to the variation of hydrophobicity of thia- and classic platforms of calixarene. For study of solubilization ability of individual macrocycles (S_{ind}) and influence of platform, we can use formula $S_{ind} = B/(\varepsilon_{ext} \cdot l)$ for the values before CAC. On this basis, it becomes clear that the aggregates based on the more hydrophobic macrocycles (thiacalixarenes) solubilize the dye more efficiently before and after CAC. Also, hydrophobic long alkyl fragments increase the solubilization capacity (Table 1).

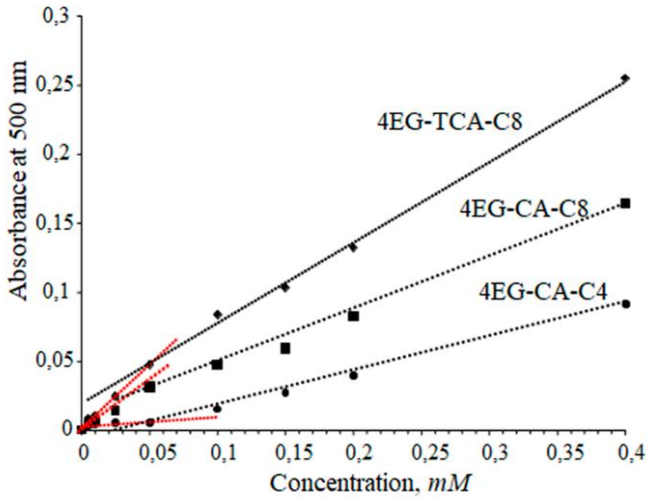

Figure 1. Plots of the dependencies of orange OT absorbance at 500 nm on the concentration of the macrocycles in aqueous solutions; *C*(macrocycles) = 0 – 0.4 mM, *C*(orange OT) = 1 mM.

Interaction of 4EG-CA-Cn and 4EG-TCA-Cn (n = 4, 8) with dianion dye- Eosin Y

The absorption spectrum of eosin Y (EY) represents an absorption maximum at 517 nm and a small shoulder at 492 nm that refers to monomeric and dimeric forms of the dye, correspondingly.[35] Figure 2A describes the effect of the macrocycles (4EG-CA-C8 as example) on the absorbance of 0.02mM EY in water. We have a possibility to observe a reduction of EY absorbance and the following shift of EY absorption maximum to higher wavelengths due to the gradual addition of surfactants. At the moment of reaching a certain concentration of the macrocycles the shift of the absorbance maximum is ceased. However, the absorbance values continued increasing till their maximum. This action indicates electrostatic interaction between EY and the macrocycle with an opposite charge.[36] The values of maximum wavelength of EY were plotted against concentration of surfactants to indicate $CAC_{abs.EY}$ (Figures 2B and 4S). The use of the sigmoidal Boltzmann-type function allowed to describe sufficiently all the plots.

An observed redshift of λ_{max} from ~517 nm to 530 nm is caused by a change of the microenvironment of the chromophore of EY due to decrease of the solution's polarity (water to surfactant) (Figure 2B).[37] And in the case of thiacalixarenes the shift is higher (up to 2–3 nm) indicating thus higher solubilization capacity of aggregates, which is consistent with the experimental data by orange OT.

For the confirmation of the interaction mechanism of macrocycles with EY, fluorescence spectroscopy was carried out. This method is the simplest for polarity studies. Figure 2C shows emission spectra of EY after adding 4EG-TCA-C8. As we can see, the surfactants before CAC quench the fluorescence of EY, that is caused by the formation of non-ionic complex of surfactant and dye due to electrostatic interaction (Figure 5S).[38] Figure 6S demonstrates the Stern–Volmer plots for all the calixarenes / thiacalixarenes – EY before CAC (before redshift). The non-linear view of the Stern-Volmer plots shows the combined static and dynamic quenching.[39] As compared to 4EG-CA-C*n*, the decrease in the emission intensity of EY was more significant with 4EG-TCA-C*n* that comes from their great hydrophobicity.

After reaching CAC the λ_{max} bathochromic shift with the further increase in the fluorescence intensity of EY is exhibited. Primarily, at a concentration before CAC, the formation of surfactant – EY ion-pairs is quenched of the EY. Nevertheless, further addition of amphiphilic macrocycles causes a change of geometry, conformation and microenvironment of EY. Subsequent surfactants self-assembly causes solubilization of EY in aggregates, which results in increase of the emission intensity.[40] Also, in the presence of aggregates, the fluorescence band of EY (EY in water maximum at λ =535 nm) shifts to 552–555 nm, as demonstrated in Figure 2C. The values of maximum wavelength of EY were plotted against concentration of surfactants to indicate $CAC_{fl.EY}$. The $CAC_{fl.EY}$ values are calculated from sigmoidal function of the Boltzmann type (Figures 2D and 7S). After CAC, adding of macrocycles did not lead to shift of EY λ_{max}. This fact indicates that the EY is solubilized in the peripheral layer of micelles and is not moved to core of the aggregates.[41]

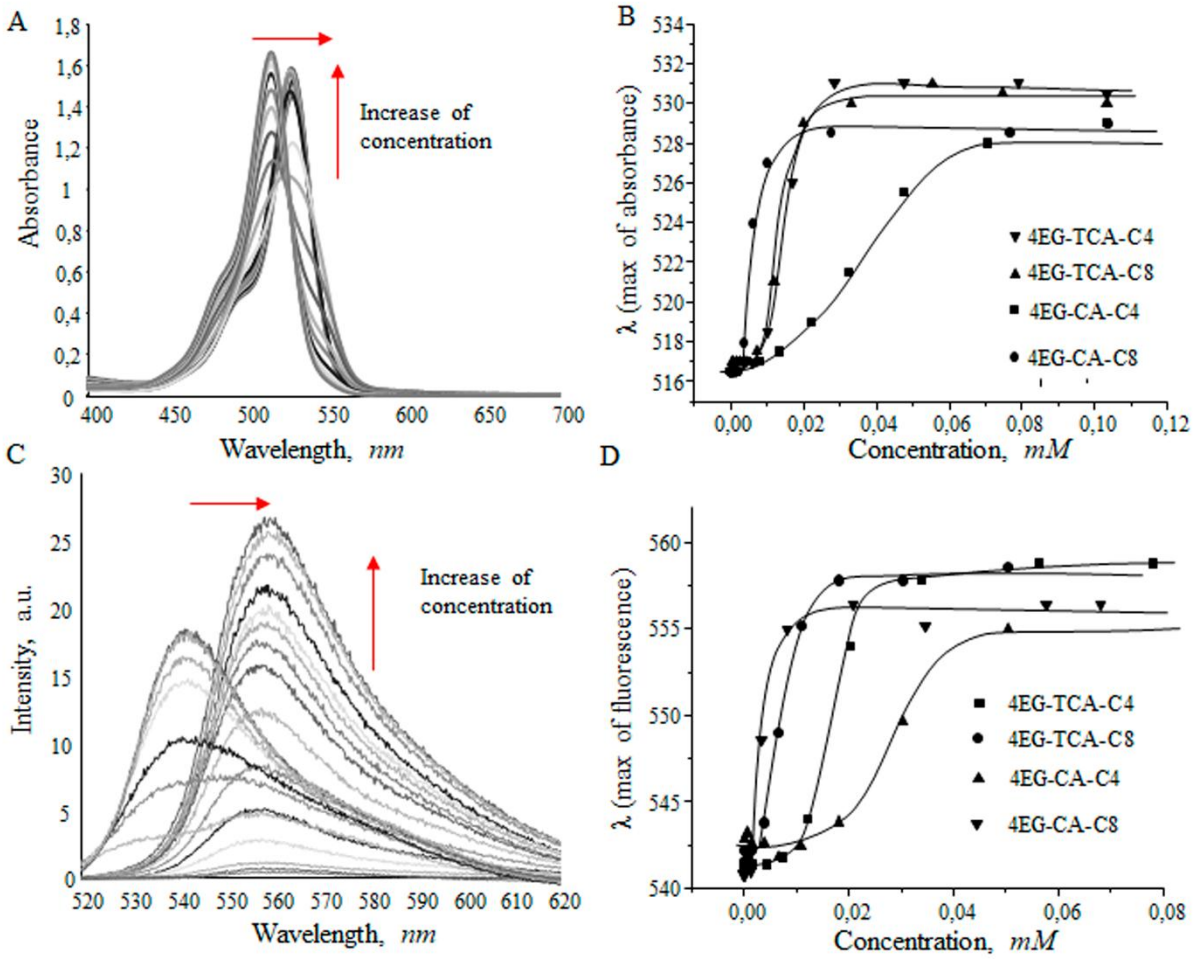

Figure 2. A) UV-vis spectra of EY in solutions of 4EG-CA-C8; B) and D) most intensive peaks wavelengths of EY in relation to macrocycles concentration in water; C) emission spectra of EY in solutions of 4EG-TCA-C8; *C*(macrocycle) = ~ 0–0.1 mM, *C*(EY) = 0.02 mM, H_2O.

Table 2. CACs of 4EG-CA-C*n* and 4EG-CA-C*n* (*n* = 4, 8) determined by EY (emission and absorbance data). Sizes of 4EG-CA-Cn and 4EG-TCA-Cn (n = 4, 8) by confocal microscopy and DLS (*C*(macrocycle) = 0.05 mM, *C*(EY) = 0.02 mM).

System	$CAC_{abs.EY}$, mM	$CAC_{fl.EY}$, mM	Size, nm	PDI	Z-average, nm
4EG-CA-C4	0.0360	0.0290	750	0.440±0.021	130±14
4EG-CA-C8	0.0054	0.0033	700	0.335±0.055	216±3
4EG-TCA-C4	0.0152	0.0171	600	0.470±0.190	470±20
4EG-TCA-C8	0.0140	0.0071	350	0.465±0.945	345±5

As can be seen from Tables 1 and 2 the intervals between the CAC_{pyr} values and $CAC_{abs.EY}/CAC_{fl.EY}$ are extremely different. Observed differences are explained by the different hydrophobicity and charge of the used dyes. The effects of negatively charged ions on the self-association of positively-charged surfactants are well-known.[42,43] Addition of counterion noticeably increases stabilization and speed of formation of the supramolecular structure. In the presence of EY the decrease of CAC is observed due to hydrophobic and *p*–*p* stacking interactions. More importantly, the interaction of dianion EY with the dicationic calixarenes led to the creation of a non-charged complex like a non-ionic surfactant. As a rule, such surfactants have lower CACs due to the lack of electrostatic repulsions.[44,45] The pyrene and orange OT interact only with hydrophobic parts of the aggregates. In summary, using pyrene and orange OT shows the real CAC value.

The sizes of forming aggregates were studied by confocal microscopy. The images of binary system EY - macrocycles with the concentration above CAC (0.05 mM) represent spherical aggregates (Figure 3, Table 2). The size of binary systems thiacalixarene – EY is smaller due to bigger interaction, which agrees well with the data of absorbance and fluorescence. Judging by the data of size we can assume that macrocycles self-assemble in aggregates containing several micelles due to ion-pair formation complex EY-macrocycle.[46,47] The DLS data

show the formation of smaller aggregates in the absence of eosin (the concentration is 1.5 times higher than CAC_{pyr}), which confirms the formation of the ion-pair formation complex EY-macrocycle. The classic calixarene are formed aggregates with smaller sizes and PDI (Table 2). The EY without surfactant is not visualized by confocal laser-scanning microscope in the same experimental settings used for the binary system (Figure S8)

Macrocycle – eosin Y systems as sensors toward adenosine phosphates

Presently, the sensing and selective recognition of charged ions by synthetic receptors attracts a significant research interest due to their potential applications in numerous areas.[48-50] Therefore, there is a strong interest in the development of artificial anion-selective sensors. The colorimetric response is a desirable characteristic of sensitive anion chemosensors.[51] One of the popular methods for recognition of molecules by calixarenes platform is an indicator displacement, where there is a change emission spectrum with competitive binding or releasing of a fluorescent probe.[52,53] This method has been used to ATP sensing using calix[5]arenes[54] or functional cyclophanes.[55] Previously, we have successfully used the systems thiacalixarene – eosin Y,[56] calix[4]arene – fluorescein[22] and polydiacetylenes[57] for detection different molecules.

Herein, we used binary system macrocycle – EY for detection anions with similar structure but with different size and charge: adenosine phosphates (AP): mono- (AMP), di- (ADP), tri- (ATP). Due to the different platforms lead to varied sensitivity of systems: thiacalixarene – eosin Y only to large molecules ATP, cone structure of calixarene to ADP and ATP (this consistent with our study by using complex calixarene-fluorescein[22]).

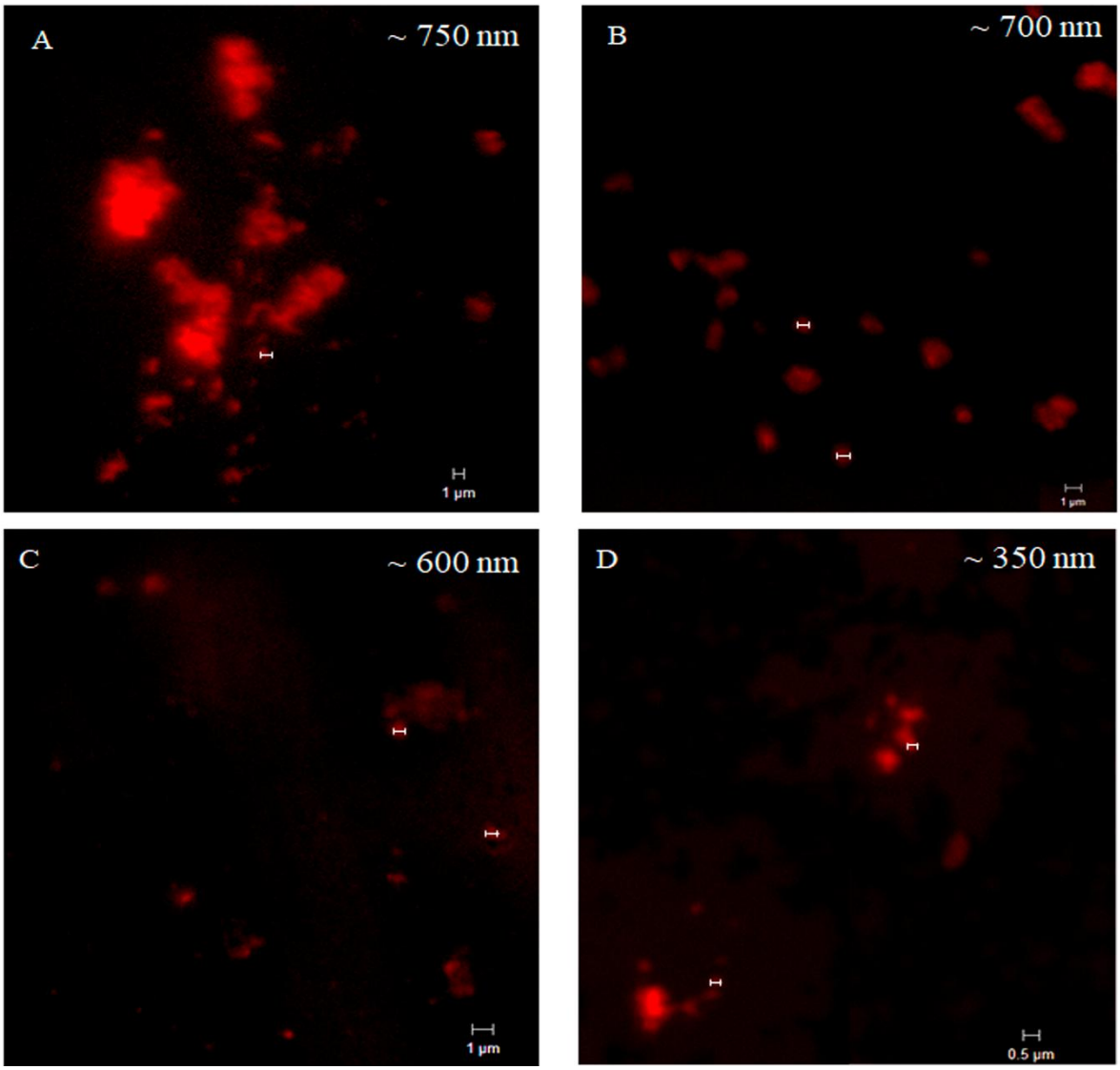

Figure 3. Images of confocal microscopy of: A) 4EG-CA-C4; B) 4EG-CA-C8; C) 4EG-TCA-C4; D) 4EG-TCA-C8; *C*(macrocycle) = 0.05 mM, *C*(EY) = 0.02 mM, H_2O.

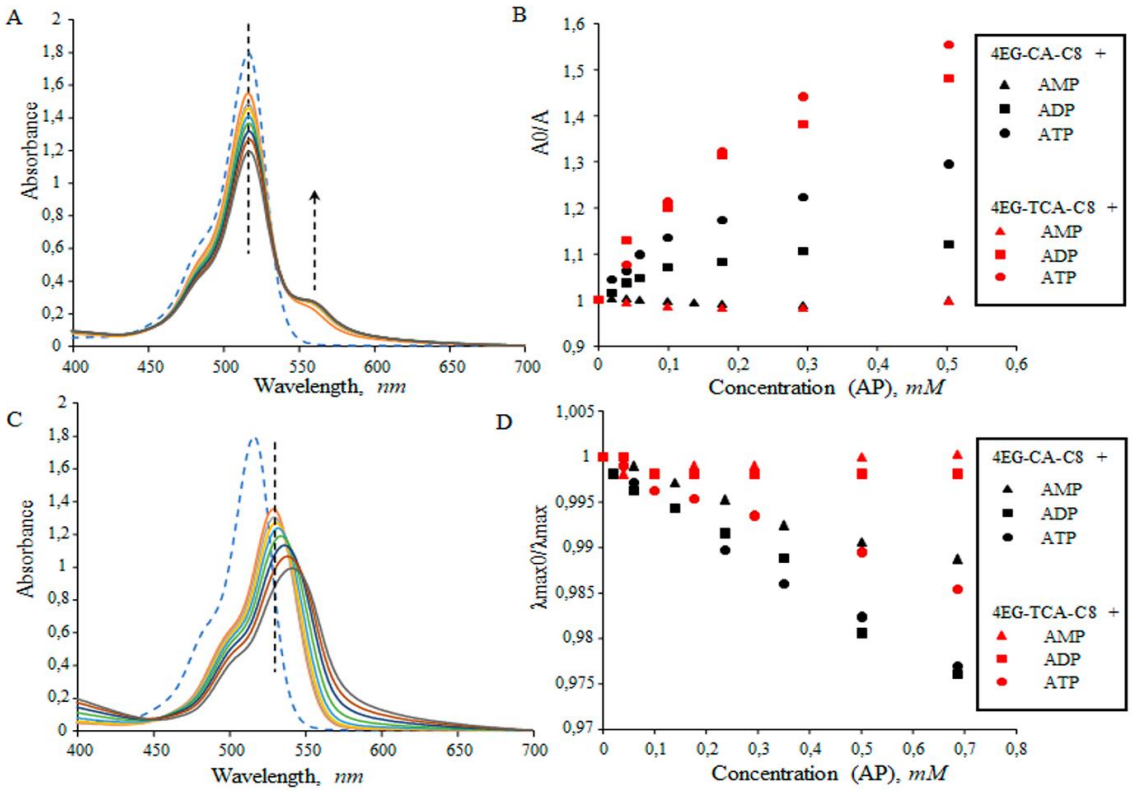

Figure 4. UV-vis spectra of: A) 4EG-CA-C8 (0.003 mM) and C) 4EG-CA-C8 (0.02 mM) – EY (0.02 mM) after addition of ATP. Dependence of: B) absorbance of EY at 517 nm and D) maxima of wavelength on the concentration of the AP in aqueous solutions of the macrocycles – EY, *C*(AP) = 0-0.7 mM, *C*(EY) = 0.02 mM (dash plot is EY in water).

Addition of the ADP and ATP to the macrocycles' solutions in concentrations lower than $CAC_{abs.EY}$ results in the quenching and appearing of the shoulder of EY spectra (Figure S9, Figure 4A,B) without shift that says about electrostatic interaction between EY and the macrocycle with an opposite charge.[35] Further, a competitive binding of ADP and ATP with positive imidazolium fragments occurs, the absorption band of EY also changes (band at 492 nm disappears) which may be attributed to the dimerization of EY induced by the formed complexes of macrocycles with AP. This is due to the reason that the complexes decreased the repulsive forces among the EY monomers and resulted in aggregation of dye monomers.[41] After addition of AMP the band intensity of EY stays unchanged (Figures S9, 4B).

Addition of ADP and ATP to the binary system 4EG-CA-C8 - EY after $CAC_{abs.EY}$ resulted with the redshift and hypochromic effect of the EY absorbance, while in the case of 4EG-TCA-C8 - EY system only ATP caused the same effect (Figure 10S, Figure 4C,D). This indicates that EY moves to the hydrophobic region of aggregates, and thiacalixarene in *1,3-alternate* form has a selectivity to ATP, whereas classic calixarene EY binds with both ADP and ATP. Obviously, this is due to different hydrophobicity and different stereoisomeric forms of platforms,[58,59] so the structure of the macrocyclic platform has a great significance: in the case of thiacalixarene – eosin Y is displaced only in the presence of a bigger multi-charged molecule (ATP). It is noteworthy that addition of ATP to pure EY (in the absence of calixarene) results in no changes in EY absorbance (Figure S11).

Color changes of binary system after addition of AP are presented in Figure 5. This is consistent with the data of UV-visible spectroscopy where 4EG-TCA-C8 after CACabs is more selective to adding ATP while adding ADP and ATP to 4EG-CA-C8 – EY led to similar changing, which is consistent with early results.

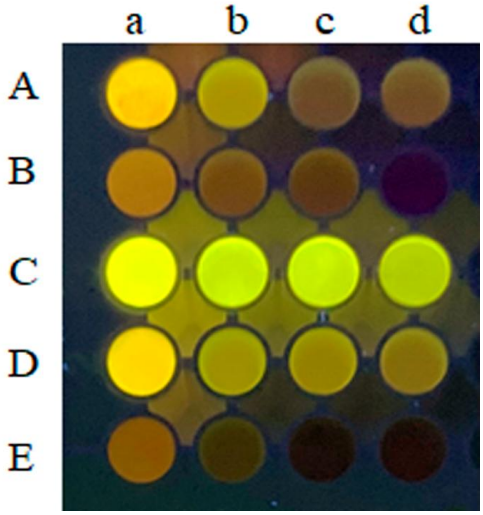

Figure 5. Photos of 4EG-TCA-C8 – EY solutions: A) before $CAC_{abs.EY}$; B) after $CAC_{abs.EY}$. Photos of 4EG-CA-C8 solutions: D) before $CAC_{abs.EY}$; E) after $CAC_{abs.\ EY}$ and C) pure EY: (a) blank (b) AMP (c) ADP (d) ATP *C*(AP) = 0.7 mM, *C*(EY) = 0.02 mM (under 365 nm lamp).

Conclusions

In summary, amphiphilic properties of N-oxyethylimidazolium-modified calixarenes in *cone* and thiacalixarene in *1,3-alternate* stereoisomeric form were studied. We used the visible absorption and / or emission of different type of dyes: eosin Y, orange OT and pyrene as probe molecules to identify the critical aggregate concentration of surfactants. The methods are based on the spectral changes in absorbance and / or fluorescence. The critical aggregate concentrations of macrocycles are calculated from the Boltzmann equation. The solubilization capacity regarding orange OT was counted for different macrocycles, where thiacalixarenes are more capacious. Due to this the surfactants with a macrocyclic platform have a potential for use in biotechnology both for the creation of delivery vehicles for hydrophobic substrates and for the creation of non-viral vectors or drug delivery systems. So, we have successfully applied a mix of eosin Y and calixarene/thiacalixarene to the recognition of adenosines by UV-vis method, and showed that the binary system of thiacalixarene – eosin Y selectively recognizes ATP, which is achieved through the better complementarity of this platform.

Acknowledgements. We thank the Russian Science Foundation for the financial support of this work (grant No. 21-73-00100).

References

1. Williams G.T., Haynes C.J.E., Fares M., Caltagirone C., Hiscock J.R., Gale P.A. *Chem. Soc. Rev.* **2021**, *50*, 2737–2763. DOI: 10.1039/D0CS00948B.
2. Washino G., Soto M.A., Wolff S., MacLachlan M.J. *Commun. Chem.* **2022**, *5*, 155. DOI: 10.1038/s42004-022-00774-5.
3. Song Q., Cheng Z., Kariuki M., Hall S.C.L., Hill S.K., Rho J.Y., Perrier S. *Chem. Rev.* **2021**, *121*, 13936–13995. DOI: 10.1021/acs.chemrev.0c01291.
4. Huang F., Anslyn E.V. *Chem. Rev.* **2015**, *115*, 6999–7000. DOI: 10.1021/acs.chemrev.5b00352
5. Kumar R., Lee Y.O., Bhalla V., Kumar M., Kim J.S. *Chem. Soc. Rev.* **2014**, *43*, 4824–4870. DOI: 10.1039/C4CS00068D.
6. Steed J.W., Turner D.R., Wallace K.J. *Core Concepts in Supramolecular Chemistry and Nanochemistry;* John Wiley: West Sussex, UK, 2007; 48–101.
7. Böhmer V. *Angew. Chem. Int. Ed.* 1995, *34*, 713–745. DOI: 10.1002/anie.199507131.
8. Gutsche C.D. *Calixarenes: an Introduction*, 2nd ed.; Royal Society of Chemistry: Cambridge, UK, **2008**. 1–276.
9. Kashapov R.R., Razuvayeva Y.S., Ziganshina A.Y., Mukhitova R.K., Sapunova A.S., Voloshina A.D., Zakharova L.Ya. *Macroheterocycles* **2019**, *12,* 346–349. DOI: 10.6060/mhc190549k.
10. Podyachev S.N., Zairov R.R., Mustafina A.R. *Molecules* **2021**, *26*, 1214. DOI: 10.3390/molecules26051214.
11. Guérineau V., Rollet M., Viel S., Lepoittevin B., Costa L., Saint–Aguet P., Laurent R., Roger Ph., Gigmes D., Martini C., Huc V. *Nat. Commun.* **2019**, *10*, 113. DOI: 10.1038/s41467-018-07751-4.
12. Guan Z.-J., Zeng J.-L., Nan Z.-A., Wan X.-K., Lin Yu-M., Wang Q.-M. *Sci. Adv.* **2016**, *2*, 1600323. DOI: 10.1126/sciadv.1600323.
13. Basilotta R., Mannino D., Filippone A., Casili G., Prestifilippo A., Colarossi L., Raciti G., Esposito E., Campolo M. *Molecules* **2021**, *26*, 3963. DOI: 10.3390/molecules26133963.
14. Razuvayeva Yu., Kashapov R., Zakharova L. Calixarene-based pure and mixed assemblies for biomedical applications. *14th International Symposium of Macrocyclic and Supramolecular Chemistry (ISMSC2019)*, Lecce, Italy, 2-6 June 2019. DOI: 10.1080/10610278.2020.1725515.
15. Isik A., Oguz M., Kocak A., Yilmaz M. *J. Incl. Phenom. Macrocycl. Chem.* **2022**, *102*, 439–449. DOI: 10.1007/s10847-022-01134-5.
16. Rathore R., Lindeman S.V., Abdelwahed S.H. *Molecules* **2022**, *27*, 5994. DOI: 10.3390/molecules27185994.
17. Pan Y.-C., Hu X.-Y., Guo D.-S. *Angew. Chem. Int. Ed.* **2021**, *60,* 2768. DOI: 10.1002/anie.201916380.
18. Mostovaya O.A., Vavilova A.A., Stoikov I.I. *Colloid J.* **2022**, *84*, 546–562. DOI: 10.1134/S1061933X22700041.
19. Giuliani M., Morbioli I., Sansone F., Casnati A. *Chem. Commun.* **2015**, *51*, 14140–14159. DOI: 10.1039/C5CC05204A.
20. Bagnacani V., Franceschi V., Fantuzzi L., Casnati A., Donofrio G., Sansone F., Ungaro R. *Bioconjugate Chem.* **2012**, *23*, 993–1002. DOI: 10.1021/bc2006829.
21. Iki N., Miyano S. *J. Inclusion Phenom.* **2001**, *41*, 99–105. DOI: 10.1023/A:1014406709512.
22. Gafiatullin B.Kh., Radaev D.D., Osipova M.V., Sultanova E.D., Burilov V.A., Solovieva S.E., Antipin I.S. *Macroheterocycles* **2021**, *14*, 171–179. DOI: 10.6060/mhc210439s.
23. Ocherednyuk E.A., Garipova R.I., Bogdanov I.M., Gafiatullin B.Kh., Sultanova E.D., Mironova D.A., Daminova A.G., Evtugyn V.G., Burilov V.A., Solovieva S.E., Antipin I.S. *Colloids Surf. A: Physicochem. Eng. Asp.* **2022**, *648*, 129236. DOI: 10.1016/j.colsurfa.2022.129236.
24. Bitter I., Csokai V. *Tetrahedron Lett*. **2003**, *44*, 2261–2265. DOI: 10.1016/S0040-4039(03)00285-5.
25. Bara J.E., Gabriel C.J., Lessmann S., Carlisle T.K, Finotello A., Gin D.L., Noble R.D. *Ind. Eng. Chem. Res.* **2007**, *46*, 5380–5386. DOI: 10.1021/ie070437g.
26. Rodik R.V., Anthony A.-S., Kalchenko V.I., Mely Y., Klymchenko A.S. *New J. Chem.* **2015**, *39*, 1654–1664. DOI: 10.1039/C4NJ01395F.
27. Kästner U., Zana R. *J. Colloid Interface Sci.* **1999**, *218*, 468–479. DOI: 10.1006/jcis.1999.6438.
28. Ruiz C.C. *Colloid Polym. Sci.* **1995**, *273*, 1033–1040. DOI: 10.1007/BF00657670.
29. Aguiar J., Carpena P., Molina-Bolıvar J.A., Ruiz C.C. *J. Colloid Interface Sci.* **2003**, *258*, 116–122. DOI: 10.1016/S0021-9797(02)00082-6.
30. Kalyanasundaram K., Thomas J.K. *J. Am. Chem. Soc.* **1977**, *99*, 2039–2044. DOI: 10.1021/ja00449a004.
31. Rigg M.W., Liu F.W.J. *J. Am. Oil Chem. Soc.* **1953**, *30,* 4–17. DOI: 10.1007/BF02639912.
32. Tehrani-Bagha A.R., Holmberg K. *Materials* **2013**, *6*, 580–608. DOI: 10.3390/ma6020580.
33. Zhiltsova E.P., Pashirova T.N., Ibatullina M.R., Lukashenko S.S., Gubaidullin A.T., Islamov D.R., Kataeva O.N., Kutyreva M.P., Zakharova L.Y. *Phys. Chem. Chem. Phys*. **2018**, *20*, 12688–12699. DOI: 10.1039/C8CP01954A
34. Ren S., Wang M., Wang C., Wang Y., Sun C., Zeng Z., Cui H., Zhao X. *Polymers* **2021**, *13*, 3307. DOI: 10.3390/polym13193307.
35. Chakraborty M., Panda A.K. *Spectrochim. Acta A Mol. Biomol. Spectrosc.* **2011**, *81*, 458–465. DOI: 10.1016/j.saa.2011.06.038.
36. Biswas S., Bhattacharya S.C., Sen P.K., Moulik S.P. *J. Photochem. Photobiol. A: Chem.* **1999**, *123*, 121–128. DOI: 10.1016/S1010-6030(99)00028-3.
37. Garg P., Kaur B., Kaur G., Saini S., Chaudhary G.R. *Colloids Surf. A: Physicochem. Eng. Asp.* 2021, *610*, 125697. DOI: 10.1016/j.colsurfa.2020.125697
38. De S., Das S., Girigoswami A. *Spectrochim. Acta A*. **2005**, *61*, 1821-1833. DOI: 10.1016/j.saa.2004.06.054.

39. Lichota A., Szabelski M., Krokosz A. *Int. J. Mol. Sci.* **2022**, *23,* 12382. DOI: 10.3390/ijms232012382.
40. Sharma R., Kamal A., Mahajan R.K. *RSC Adv.* **2016**, *6*, 71692–71704. DOI: 10.1039/C6RA12056C
41. Hwang D., Ramsey J.D., Kabanov A.V. *Adv Drug Deliv Rev.* **2020**, 156*,* 80–118. DOI: 10.1016/j.addr.2020.09.009.
42. Wang D.-X., Wang M.-X. *Acc. Chem. Res.* **2020**, *53,* 1364–1380. DOI: 10.1021/acs.accounts.0c00243.
43. Kashapov R.R., Kharlamov S.V., Sultanova E.D., Mukhitova R.K., Kudryashova Y.R., Zakharova L.Y., Ziganshina A.Y., Konovalov A.I. *Chem. Eur. J.* **2014**, *20*, 14018–14025. DOI: 10.1002/chem.201403721.
44. Castaldi M., Costantino L., Ortona O., Paduano L., Vitagliano V. *Langmuir* **1998**, *14*, 5994–5998. DOI: 10.1021/ la980457a.
45. Burilov V.A., Fatikhova G.A., Dokuchaeva M.N., Nugmanov R.I., Mironova D.A., Dorovatovskii P.V., Khrustalev V.N., Solovieva S.E., Antipin I.S. *Beilstein J. Org. Chem.* **2018**, *14*, 1980–1993. DOI: 10.3762/bjoc.14.173.
46. Rodik R.V., Cherenok S.O., Postupalenko V.Y., Oncul S., Brusianska V., Borysko P., Kalchenko V.I., Mely Y., Klymchenko A.S. *J. Colloid Interface Sci.* **2022**, *624*, 270–278. DOI: 10.1016/j.jcis.2022.05.124.
47. Wang J., Ding X., Guo X. *Adv. Colloid Interface Sci.* **2019**, *269,* 187–202. DOI: 10.1016/j.cis.2019.04.004.
48. Zhou W.-L., Lin W., Chena Y., Liu Y. *Chem. Sci*. **2022**, *13*, 7976–7989. DOI: 10.1039/D2SC01770A
49. Patel N., Nandan P., Kumbhani J., Bhatt K., Modi K. *Med. Analy. Chem. Int. J.* **2020**, *4,* 000162. DOI: 10.23880/macij-16000162.
50. Kuswandi B., N/a N., Verboom W., Reinhoudt D.N. *Sensors* **2006**, *6*, 978–1017. DOI: 10.3390/s6080978.
51. Rahman Sh., Tomiyasu H., Wang Ch.-Z., Georghiou P.E., Alodhayb A., Carpenter-Warren C.L., Elsegood M.R.J., Teat S.J., Redshaw C., Yamato T. *New J. Chem.* **2021**, *45*, 19235–19243. DOI: 10.1039/D1NJ02991F.
52. Wu J., Kwon B., Liu W., Anslyn E.V., Wang P., Kim J.S. *Chem. Rev.* **2015**, *115*, 7893–7943. DOI: 10.1021/cr500553d.
53. You L., Zha D., Anslyn E.V. *Chem. Rev.* **2015**, *115,* 7840–7892. DOI: 10.1021/cr5005524.
54. Bojtár M., Kozma J., Szakács Z., Hessz D., Kubinyi M., Bitter I. *Sens. Actuators, B* **2017**, *248*, 305–310. DOI: 10.1016/j.snb.2017.03.163.
55. Ramaiah D., Neelakandan P.P., Nair A.K., Avirah R.R. *Chem. Soc. Rev.* **2010**, *39*, 4158–4168. DOI: 10.1039/ B920032K.
56. Burilov V.A., Mironova D.A., Ibragimova R.R., Nugmanov R.I., Solovieva S.E., Antipin I.S. *Colloids Surf. A: Physicochem. Eng. Asp.* **2017**, *515*, 41–49. DOI: 10.1016/ j.colsurfa.2016.12.007.
57. Sultanova E.D., Gazalieva A.M., Makarov E.G., Belov R.N., Evtugyn V.G., Burilov V.A., Solovieva S.E., Antipin I.S. *Colloids Surf. A: Physicochem. Eng. Asp.* **2021**, *630*, 127642. DOI: 10.1016/j.colsurfa.2021.127642.
58. Kumar R., Sharma A., Singh H., Suating P., Kim H.S., Sunwoo K., Shim I., Gibb B.C., Kim J.S. *Chem. Rev.* **2019**, *119*, 9657–9721. DOI: 10.1021/acs.chemrev.8b00605.
59. Zhao M., Lv J., Guo D.-Sh. *RSC Adv.* **2017**, *7*, 10021–10050. DOI: 10.1039/C6RA25616C.

Received 24.04.2023
Accepted 03.05.2023